

# Mechanochemical changes in absorption and fluorescence of DDM-containing epoxies



Ryan Toivola <sup>a,\*</sup>, Sei-Hum Jang <sup>a</sup>, Donald Mannikko <sup>b</sup>, Stefan Stoll <sup>b</sup>, Alex K-Y. Jen <sup>a,b</sup>, Brian D. Flinn <sup>a</sup>

<sup>a</sup> Department of Materials Science & Engineering, University of Washington, Seattle, WA, USA

<sup>b</sup> Department of Chemistry, University of Washington, Seattle, WA, USA

## ARTICLE INFO

### Article history:

Received 29 December 2017

Received in revised form

13 March 2018

Accepted 14 March 2018

Available online 16 March 2018

### Keywords:

Epoxy

Mechanochromism

Fluorescence

## ABSTRACT

Mechanochemical changes in absorption or fluorescence in solid polymers are important for the development of new methods of damage sensing, and must be demonstrated in structural polymers such as epoxies for widespread use. With this in mind, we have observed that diamine-cured epoxies containing 4,4'-diaminodiphenyl methane (DDM) framework display mechanochemical changes in both absorption and fluorescence. Samples change from original “blue” to mechanochemically activated “red” fluorescence in response to uniaxial compressive deformation beginning in the early stages of strain hardening. Accompanying the “red” fluorescence is an increase in radical concentration; both are impermanent in time, suggesting the reactive intermediate as the fluorophore. Orange and green chromophores are generated by compression as well; the orange chromophore is the red-emitting fluorophore while the green chromophore is non-fluorescent at ambient conditions. Our work indicates that the DDM structure is the origin of the mechanochromic responses, and stoichiometric variation and degree of cure are strong determinants for whether orange or green chromophores will form. Based on these results the red-emitting orange chromophore is proposed as a reactive radical intermediate of core DDM structure, generated by bond scission reactions on the epoxy network. The green chromophore is a quinoidal methine resulting from the intermediates.

© 2018 Elsevier Ltd. All rights reserved.

## 1. Introduction

Within the field of stimuli-responsive polymers, those that have an optical response to mechanical force are especially interesting. Two examples of this are mechanochromism (force-induced color change, MC) and mechanoresponsive fluorescence (force-induced change in fluorescent emission characteristics, MRF), with recent developments suggesting potential applications in damage detection, non-destructive evaluation, and strain sensing [1,2]. Most of the examples of MC/MRF changes in solid polymer systems have been realized in ‘soft’ polymers with low modulus and high elongation at break, requiring large amounts of deformation to effect the change [3–6]. It is important that MC/MRF systems be identified or developed in strong, stiff polymers as these are used in structural applications that will have the most critical need for damage detection capability.

An especially useful solid polymer is diamine-cured epoxy, a glassy amorphous thermoset with mechanical properties sufficient for use in structural applications. Epoxies are used in the aerospace, marine, and automotive industries as the matrix material for fiber-reinforced composites [7,8]; in the electronics industry as encapsulants; and in myriad applications as structural adhesives. Recently, our group and others have worked to develop MC/MRF sensor systems that are active in epoxy polymers [9–13]. Most of these efforts have tried to impart MC/MRF functionality to epoxies by incorporating secondary mechanochemically active molecules into the thermoset network. However, in one example we found that a commercially available epoxy based on 4,4'-tetra-glycidyl diaminodiphenyl methane (TGDDM) cured with diethylenetriamine (DETA) demonstrated MC/MRF behavior intrinsically, and we demonstrated its utility as an impact damage detection system for aerospace composites [10]. This work explores the origin and properties of this intrinsic MC/MRF phenomenon.

Initially, most diamine-cured epoxies are optically transparent or pale yellow in color, and emit blue fluorescence in response to

\* Corresponding author.

E-mail address: [toivore@uw.edu](mailto:toivore@uw.edu) (R. Toivola).

ultraviolet (UV) excitation. Color change in epoxies in response to external stimuli has been observed in response to mechanical force, oxygen environments, high temperatures, irradiation with gamma rays, or UV photons [14–20]. The reported colors have been yellow, brown, dark blue or green, and are often transient or reversible with specific thermal/environmental exposures. Yellow and brown colors have been positively attributed to formation of carbonyl products due to photo- or thermo-oxidation [21]. Green and blue colors have been observed in several epoxy formulations containing TGDDM or the curing agent 4,4'-diaminodiphenyl methane (DDM) in response to high temperature and UV exposure [14–16,22]. The mechanochromic generation of green color in DGEBA resin cured with 4,4'-diaminophenyl disulfide has been reported by Ruiz de Luzuriaga and co-workers [20].

Observations of a fluorescent response in epoxy to an external stimulus have been rare, and generally limited to enhancement or quenching of the intrinsic blue fluorescence rather than the creation of new fluorophores. Levy and Ames studied the viscosity dependence of the fluorescence of TGDDM-based epoxy formulations. They noted a broad fluorescence at 463 nm that was viscosity dependent and that was correlated with the TGDDM monomer [23–25]. They observed a sharp fluorescence peak at ~606 nm in an uncured TGDDM resin but did not speculate on its origin or stimuli dependence [23]. Our previous work observed that compression or impact of cured TGDDM-DETA samples produced a similar red-emitting fluorescent species with emission maximum at 607 nm, which we believe was the first reporting of intrinsic MRF in epoxy [10].

Excluding carbonyl formation, nearly all of the stimuli-responsive color change and fluorescence observations in epoxy have implicated DDM as the responsive structure, whether it is contained in the TGDDM epoxy monomer or the DDM amine monomer. While the mechanisms and schemes have varied, the proposed green chromophore-generating transition is often from 'benzoidal methane' DDM to a green or dark blue 'quinoidal methine' chromophore derived from DDM [14–16,19,22]. The proposed reaction pathways have involved bond scission or hydrogen abstraction at one of several vulnerable bonds including the C-N bond near crosslink sites and the C-H bond at the central DDM methylene. These attacks generate several proposed reactive intermediates, some of which result in quinoidal methines.

The reactive intermediates between the initial DDM structure and the ultimate products of a bond scission or hydrogen abstraction event have not been previously studied in great detail. The proposed intermediates are "open-shell" molecules similar to diphenylmethyl and triphenylmethyl radicals which exhibit fluorescent emission, with large Stokes shifts and often in the red wavelengths, when stabilized long enough for study [26,27]. Reactive intermediates may be rendered persistent by immobilizing them via cryogenic solvent glass (matrix isolation technique), trapping in zeolite channels, or by hosting the parent molecule in a polymer solid and creating the intermediate via irradiation [28–31]. In comparison with these techniques, the glassy amorphous epoxy network may be an ideal environment for prolonging the lifetime of a reactive intermediate enough to observe its fluorescence. Previous works have used electron paramagnetic resonance (EPR) spectroscopy to confirm and correlate the formation of green chromophores with radicals produced in DDM-containing epoxies by external stimuli, although the lack of hyperfine structure did not allow conclusive identification of the radical species [14,16].

Molecules similar to DDM that form a green chromophore through transition from benzoidal methane to quinoidal methine form include Wurster's Blue and Malachite Green dyes [32–34]. An

interesting study on mechanochemical generation of radical derivative of viologen, a related molecule with multiple redox states, has been reported recently, showing that the viologen derivative in powder form turned from yellow to green under 1–3 GPa of compression or hydrostatic pressure; detailed absorbance studies in a diamond anvil cell showed the formation of a red-colored radical chromophore during the loading period of a pressure cycle, with the radical stabilizing to a green-colored form during the unloading period [35]. Molecules which transition from one emissive state to another via rearrangement of covalent bonds have found application in bioimaging [36].

The relationship between mechanochemical and photochemical reactions is quite interesting. A well-known class of mechanochemical reactions is based on the ring-opening of cyclobutenes [37–39]; this electrocyclic reaction can also be activated by incident photons [40–42]. Several mechanochemical reactions producing MC/MRF response can also be accomplished photochemically. The seminal spiropyran-merocyanine system displays both mechanochromic and photochromic responses; the ring-opening reaction from weakly colored, non-emissive spiropyran form to colorful, emissive merocyanine form can be produced by applying mechanical force [2] or by irradiation with ultraviolet light [43–46]. The colorless dimer of lophine (2,4,5-triphenylimidazolyl) can also be dissociated into colorful radical monomers mechanochemically via ultrasonication of polymer chains or grinding of purified powders, or photochemically by irradiation with 365 nm photons [47–49]. The study of molecular systems that are both mechanochemically and photochemically active has potential to advance the understanding of both fields, with researchers choosing the most appropriate method to generate and quantify mechano- and photochemical phenomena.

In this work we report on the MC/MRF response of DDM-containing epoxies under uniaxial compression. Diamine-cured solid epoxies containing DDM from either the epoxy or diamine monomer display an irreversible "blue-to-red" change in fluorescent emission, along with the generation of orange or green chromophores, in response to uniaxial compression. Our experiments show the "red" fluorescence results from the orange chromophore, which is a reactive radical intermediate of the DDM aromatic core that can turn to non-emissive forms including the green chromophore, a quinoidal methine. In a companion work to this paper, we show that sustained UV illumination of DDM-containing epoxies also produces these optical changes.

## 2. Experimental

### 2.1. Materials

The molecular structures of the commercially available epoxies and diamine curing agents used in this study are shown in Fig. 1. These epoxies and curing agents can be used in different combinations to produce solid polymers with a wide variety of thermal and structural properties. The tetra-functional TGDDM epoxy used in this study was obtained from Huntsman under the product name MY720. The di-functional diglycidyl ether of bisphenol A (DGEBA) was obtained from Miller-Stephenson under the trade name Epon 828. The long-chain epoxy diluent diglycidyl ether of polypropylene glycol (DGEPPG) was obtained from Dow Chemical under the trade name DER 736. The DETA, DDM, and 4,4'-methylenebis (2-methylcyclohexylamine) (MMCA) curing agents were obtained from Sigma Aldrich. The 4,4'-diaminodiphenyl sulfone (DDS) curing agent was obtained from Huntsman. The polyoxypropylenediamine (POPDA) curing agent was obtained from Dow under the trade name Epikure 3274.

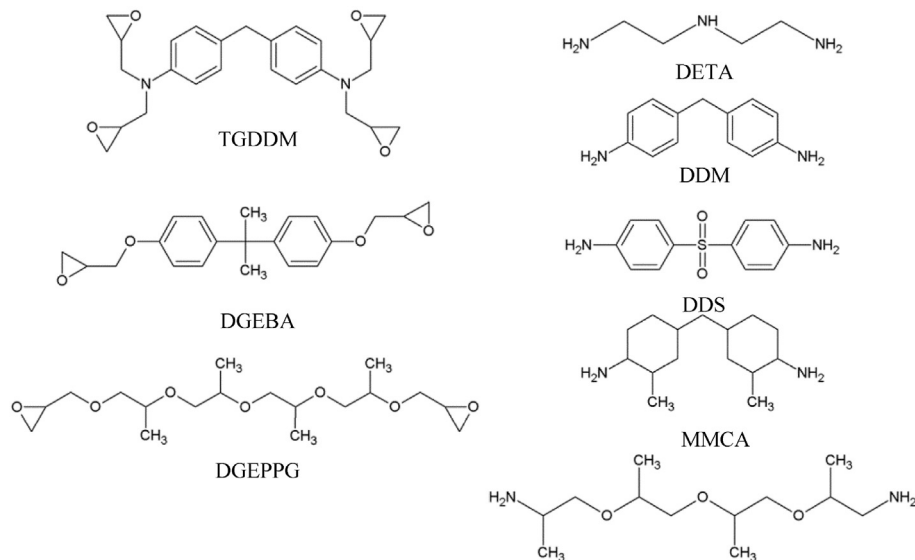


Fig. 1. Molecular structures of epoxy monomers and curing agents used in this study. Epoxies at left; diamine curing agents at right.

## 2.2. Sample fabrication and thermal analysis

All three epoxies are liquid at room temperature; TGDDM has high viscosity and was raised to 70 °C for pouring and weighing, but cooled to room temperature before mixing. The DETA, MMCA, and POPDA curing agents are also liquids at room temperature, so formulations involving these three curing agents were mixed with the epoxies in 25–40 g batches and poured into aluminum molds to cure. The DDM curing agent was obtained in solid pellets, which were heated until melting then mixed into the epoxies as liquids. The DDM returned to solid form during mixing, so the mixture was gently heated until the DDM crystals dissolved, then returned to room temperature. The DDS curing agent was obtained in powder form. The powdered DDS was stirred into the epoxy liquids which were gently heated until the DDS powder melted, after which the liquids were stirred and removed from heat.

Dynamic differential scanning calorimetry (DSC) was used to determine the appropriate cure temperatures of the various epoxy samples. The onset of the cure exotherm in a dynamic DSC scan at 5 °C per minute was used as the cure temperature; samples were cured for 1 h at this temperature in a ThermoFisher HeraTherm convection oven. These cure schedules produced solid epoxy casts that were capable of undergoing machining and testing, but were not necessarily completely cured. For the detailed study of TGDDM-POPDA, dynamic DSC was used to determine the degree of cure (d.o.c.) and the glass transition temperature ( $T_g$ ) of the different TGDDM-POPDA stoichiometries and cure conditions.

Samples of 5–15 mg in mass were scanned at 5 °C per minute from room temperature through a temperature range encompassing the cure reaction, in a TA Instruments Q50 DSC. The d.o.c. was calculated using equation (1)

$$d.o.c = 1 - \frac{\Delta H_{res}}{\Delta H_{rxn}} \quad (1)$$

Where  $\Delta H_{res}$  is the residual heat of reaction given off by the sample during a scan after the cure process, and  $\Delta H_{rxn}$  is the total heat of reaction given off by the mixture during a scan before cure. The heats of reaction were determined by integrating under the reaction curve using the TA Universal Analysis software. Samples were

assigned a d.o.c. of 1 if no  $\Delta H_{res}$  was measurable, although the increasing  $T_g$  after higher-temperature cure processes suggests that at least some crosslink sites are still available. Glass transition temperatures were also determined using the software, which identified the characteristic step in the heat flow curve associated with  $T_g$ . Samples with low d.o.c. often have a  $T_g$  below room temperature, and these are not assigned a  $T_g$  value.

For detailed study of the TGDDM-POPDA system, batches of epoxy with three stoichiometric conditions were mixed. Formulation **A** had a 50 wt% excess of the TGDDM epoxy; formulation **B** was stoichiometrically balanced, for a ratio of 1 epoxide group to 1 amine group of curing agent; formulation **C** had a 50 wt% excess of POPDA amine curing agent. Samples were mixed at room temperature, poured into molds, and left at room temperature for 24 h. The mixture was then heated in a convection oven at 50 °C for 1 h (condition 0). Prism samples of 4 mm × 4 mm by 40 mm were machined from the casts using a PACE Pico 150 low speed saw with polycrystalline diamond wafering blade. These prisms were post-cured for 30 min at 75, 100, 125, or 150 °C (conditions 1, 2, 3, and 4, respectively), then samples were machined from them for compression testing.

Samples for uniaxial compression and optical analysis were machined from the casts into flat plates of approximate dimension 4 mm × 4 mm × 1.0 mm. For transfectance baseline measurements, the samples were 0.5 mm to more closely match the path length of samples after extensive compressive deformation.

## 2.3. Mechanical deformation

Samples were compressed uniaxially in an Instron 5500R test frame between polished steel platens. Engineering stress-strain curves were determined using crosshead displacement and the load recorded by a 100 kN load cell; true stress-strain curves were determined from the engineering stress-strain data using equations (2) and (3)

$$\sigma_{true} = \epsilon_{engr} (1 + \sigma_{engr}) \quad (2)$$

$$\epsilon_{true} = \ln(1 + \epsilon_{engr}) \quad (3)$$

Samples were deformed at a crosshead displacement speed of

0.5 mm/min and were unloaded slowly, controlling the crosshead by hand, to avoid catastrophic fracture on unloading.

#### 2.4. Optical imaging and spectral analysis

Images of samples were collected using a Canon PowerShot ELPH 100HS digital camera mounted on a small tripod. Natural light images were taken in 'portrait' mode with no flash using a white ceramic plate as background. Fluorescence images were collected in 'long shutter' mode using a 15 s exposure in a darkroom using a black, nonfluorescent felt cloth as background. Illumination for the images came from a standard long wave UV bulb ( $\lambda_{\text{max}} \sim 365$  nm) mounted at  $45^\circ$  to the sample surface.

Fluorescent excitation and emission spectra were collected from samples of TGDDM-DETA polymer. The solid polymer was machined as described above into  $4 \text{ mm} \times 4 \text{ mm} \times 1 \text{ mm}$  samples and mounted into a solid sample holding fixture. Spectra were collected in a Perkin Elmer LS-50B luminescence spectrometer; spectra from samples after compression were collected within 20 min of compressive unloading.

Fluorescent emission spectra for this work were also collected with a Y-type 7-around-1 fiber optic fluorescence probe held at  $45^\circ$  to the sample surface and processed by a portable spectrometer (Stellarnet BLUE-Wave UVN 200). The excitation light was produced by an LED source (Stellarnet SL1-LED) using a 390 nm LED bulb. Measurements of changes in the fluorescent signal with time were collected using the spectrometer's episodic data capture function. To collect time-resolved emission spectra at temperatures other than room temperature, samples were attached to the digitally controlled temperature stage of a GladiATR attachment (PIKE Technologies) to a Vertex 70 spectrometer (Bruker). Samples were

brought into thermal equilibrium with a thin layer of thermally conductive paste (Arctic Silver) at room temperature; the stage was set to the desired temperature and measurements began when the temperature was reached.

Absorbance spectra were collected from solid samples using a transmittance method. A reflectance probe mounted into a  $90^\circ$  holder (Ocean Optics CSH) which isolated the probe and sample from ambient light was used to pass white light from a tungsten-halogen source (Stellarnet SL1) through the sample to a reflective aluminum foil tape layer. Light returning through the sample, having passed through the sample for a path length of twice the sample thickness, was collected by a spectrometer (Stellarnet Silver Nova). A white-light baseline value was collected with no sample in place, and absorbance spectra were determined by comparison.

Absorbance spectra from liquid samples were collected using a Thermo Fisher Evolution 300 UV-Vis spectrophotometer. Liquid solutions of epoxy dissolved in dichloromethane were held in the beam path in quartz cuvettes, and compared to baselines of pure dichloromethane liquid.

Electron paramagnetic resonance spectra were collected from compressed epoxy samples using a Bruker EMX EPR spectrometer with 1 mW of microwave (9.27138 GHz) power and a modulation amplitude of 1 G. A quartz sample tube was filled with fragments of several TGDDM-DETA samples that had been compressed to  $\sim 7$  GPa of true stress. The initial spectrum was collected  $\sim 1$  h after compression. The sample tube was kept in approximately the same alignment in the instrument at room temperature while subsequent spectra were collected for the next several days. The radical concentration was calculated by double integration of the EPR spectra.

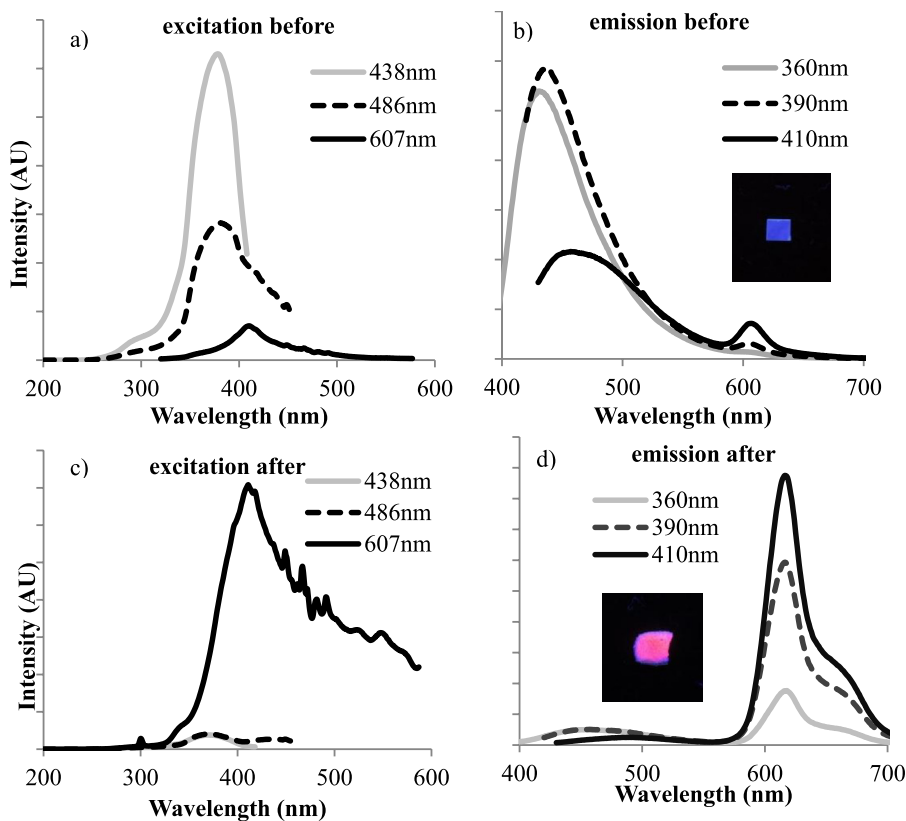


**Fig. 2.** Fluorescent properties of TGDDM-DETA epoxy before and after compression. a) Excitation spectra before compression corresponding to emission peaks at 438, 486, and 607 nm b) Emission spectra before compression due to excitation at 360, 390, 410 nm c) Excitation spectra after compression corresponding to emission peaks at 438, 486, 607 nm d) Emission spectra after compression due to excitation at 360, 390, 410 nm.

### 3. Results

#### 3.1. Excitation and emission of “blue” and “red” fluorescence

Before compression, the studied epoxy samples emit a “blue” fluorescence in response to UV excitation light, with two peaks at ~430–450 nm and ~480–500 nm depending on formulation. In previous works this emission has been attributed to the monomer components of the formulation. [18,23–25,50,51]. UV-excited blue fluorescence has been observed from epoxide monomers such as TGDDM and from diamine curing agents such as POPDA when in solid environments. Aromatic monomer components may also form excimer complexes that emit blue fluorescence. After compression however, some of the tested formulations show a dramatic “blue-to-red” change in emission response to UV light. Fig. 2 shows the excitation and emission spectra for a TGDDM-DETA sample, before and after compression to ~7 GPa of true stress. Inset to the emission spectra are fluorescent images of a TGDDM-DETA samples under long wave UV light before and after compression, showing the “blue” fluorescence before compression and “red” fluorescence after. The fluorescence has three emission peaks at 438, 486, and 607 nm. Fig. 2a shows the excitation spectra corresponding to the observed emission peaks. The excitation spectra for 438 and 486 nm are similar, a smooth peak at ~375 nm with a shoulder at ~300 nm. The excitation spectrum for 607 nm emission has a much more distinct spectrum with a broad peak at 410 nm, and several smaller peaks between 450 and 490 nm. Fig. 2b shows the three emission peaks observed using excitation of 360, 390, and 410 nm; the emission at 438 nm is stronger at lower excitation wavelengths while the emission at 486 nm is stronger at 410 nm. The 607 nm emission is observable at 390 nm and strongest at 410 nm. After compression, the excitation spectra undergo dramatic changes, as shown in Fig. 2c. The excitation corresponding to 607 nm emission shows an increase of 100-fold or more in the 410 nm peak after compression. The emission spectra after compression, shown in Fig. 2d, exhibit a corresponding change. The “red” emission at 607 nm increases in intensity due to compression, as much as 100–200-fold depending on excitation wavelength; it is

also possible to observe a potential second peak that presents as a shoulder at ~660 nm that also becomes more intense due to compression. The correlation between 410 nm excitation and 607 nm emission and their synchronized increase in response to compressive stress indicates that both can be attributed to some mechanically generated species.

#### 3.2. Identification of DDM as active structure

We performed a canvass of the 15 combinations of epoxy and diamine monomers from Fig. 1, and tested them using 1.5 GPa of uniaxial compression. Images of the samples before and after compression are shown in Fig. 3. The ambient-light images show that development of either green or orange color occurred after compression in formulations containing either the TGDDM epoxy or the DDM curing agent. Formulations that contained neither TGDDM nor DDM did not show changes in color due to compression. The colors formed were transient, fading from the sample in several hours or days at room temperature in air. The fluorescence images, taken using long-wave UV excitation, show that “red” fluorescence developed due to compression in nearly all formulations that contained either TGDDM or DDM, and did not develop in formulations that did not. The only exception occurred in TGDDM-DDS formulation, which developed green color but did not exhibit visible “red” fluorescence. These results clearly support the involvement of the DDM framework in the reaction mechanism for MC/MRF phenomena in epoxies.

#### 3.3. Fluorescent response to varying deformations

The “blue-to-red” change in fluorescence due to uniaxial compression is incremental - increasing deformation causes a stronger “red” response. The excitation spectra in Fig. 2 show that both “blue” and “red” fluorescence can be excited by 350–410 nm photons. A 390 nm LED is capable of exciting all fluorescent emission, and can be used to observe all three peaks simultaneously. This enabled comparison between samples of varying deformations and changing geometries by normalizing to the intensity of the

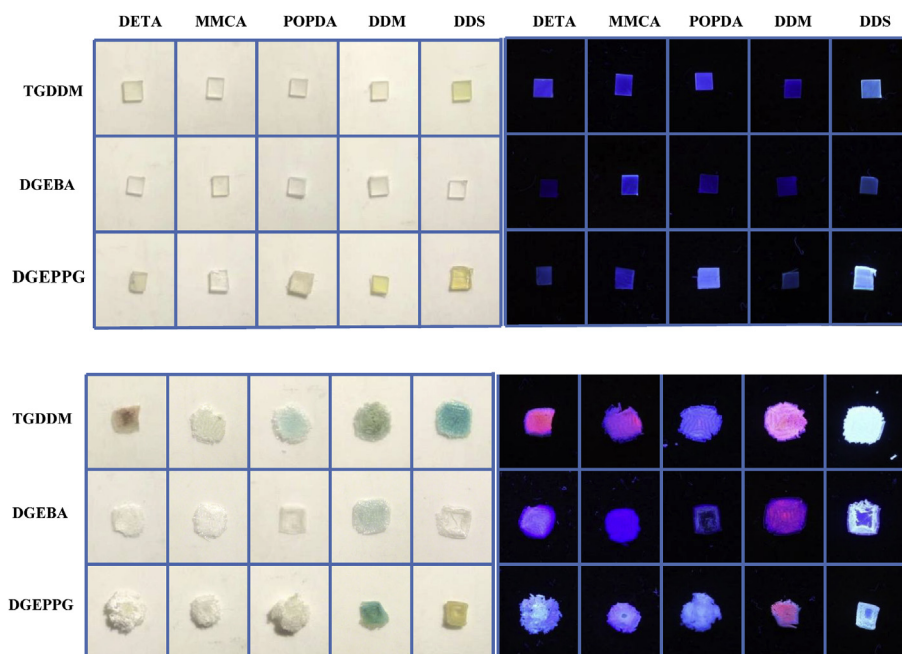


Fig. 3. Images of epoxy formulations before (top) and after (bottom) uniaxial compression. Row labels indicate epoxy component; column labels indicate amine curing agent component. Left grid - ambient light. Right grid - long wave UV light.

486 nm emission peak.

The normalized fluorescence spectra collected from samples of TGDDM-DETA immediately after compressions of varying maximum true stress are shown in Fig. 4. The inset shows the low-intensity regions of the spectra, an expansion of the dotted box in the large plot. After compression the 438 nm “blue” peak emission is decreased slightly and the 607 nm “red” peak emission becomes dramatically more intense. This peak grows stronger with increasing compressive deformation.

Examination of the mechanical deformation characteristics via the stress-strain curves of samples during compression can help to determine details of the activation mechanism. The true stress-true strain curves of the three epoxies cured with DDM curing agent are shown in Fig. 5a. Inset to Fig. 5a is a magnified view of the yielding and strain-softening region, an expansion of the dotted box in the main figure, with labels indicating the elastic modulus and yield strength of the samples. Fig. 5b shows the intensity of 607 nm fluorescence plotted against the maximum true stress for several samples of these three DDM cured epoxies. The fluorescence has been normalized to facilitate comparison using Equation (4)

$$I^* = \frac{I - I_{\text{initial}}}{I_{\text{maximum}} - I_{\text{initial}}} \quad (4)$$

where  $I^*$  is the plotted intensity,  $I$  is the measured intensity,  $I_{\text{initial}}$  is the intensity measured from a sample before deformation, and  $I_{\text{maximum}}$  is the highest intensity measured after compression from the formulation being plotted. The onset of activation for each formulation is determined by the x-intercept of the line fitted to the activation region of each formulation in this plot.

The TGDDM-DDM and DGEBA-DDM samples are rigid glasses, with high moduli and yield strengths, while the DGEPPG-DDM sample is more flexible with much lower modulus and yield strength. However, the activation onset for all three occurs at similar stress levels, between 1.2 and 2.1 GPa. This stress level occurs in the early-to-middle of the strain hardening region of the true stress-true strain curve, and has been marked with a bracket in Fig. 10. This level of deformation is consistent with fluorescence activation conditions we previously observed in TGDDM-DETA [10]. The similarity of the activation onset behavior across all three formulations suggests that a mechanism common to all three is responsible for fluorescent species generation; the only common structure in the formulations is the DDM framework, further evidence for its involvement in the mechanochemical creation of the

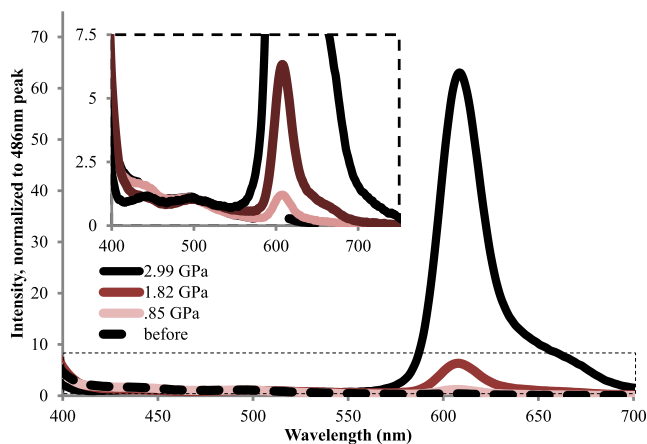


Fig. 4. Fluorescence emission after compression. TGDDM-DETA samples to varying compressive true stress levels. Inset: magnified plot of low-intensity region. Spectra normalized to 486 nm emission peak.

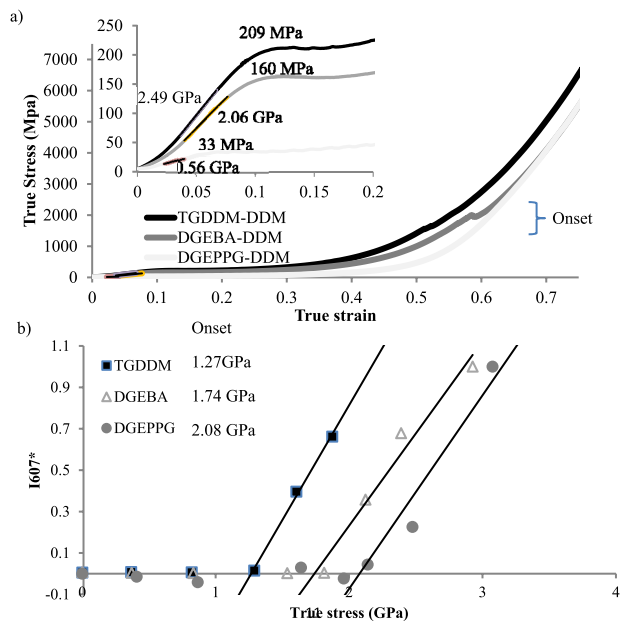


Fig. 5. a) True stress-true strain curve of DDM-cured epoxy formulations. Inset - yielding/strain softening region. b) Normalized 607 nm emission intensity vs true stress for DDM-cured epoxy formulations.

fluorophore.

In TGDDM and DGEBA samples, macroscopic fracture caused a response significant enough to be observed on the stress-strain plot in Fig. 5 (~1.54 GPa for TGDDM; ~1.98 GPa for DGEBA). The onset of fluorescent activation occurs at true stress levels slightly lower than those causing macroscopic fracture in these two formulations. Other researchers have established that covalent bond scission events are strongly correlated with macroscopic fracture, with scission often preceding fracture in samples subjected to increasing stress [52–57]. Recent quantum mechanics/molecular mechanics simulation work by Barr et al on the DGEBA-DDM system have determined the uniaxial compression stress required for scission of the first-to-break covalent bond to be 1.10–1.25 GPa, which is in close agreement with the activation onset of our samples [58]. These results suggest a link between bond scission and fluorescent activation in our samples.

The correlation between bond scission-causing stresses and fluorescent activation in our samples naturally suggests the involvement of a radical species created via rupture of a covalent bond. The mechanochemical creation of unstable radicals has been observed often in solids and polymers, and has been accompanied by color change in several instances [49,59–62]. Some radical species especially those involving aromatic rings, such as diphenylmethyl, are quite strongly fluorescent [63–71]. Most radicals, however, are inherently unstable intermediates which rapidly form more stable products. The optical properties of fluorescent radical intermediates can be difficult to observe in general due to their reactivity and very short lifetime in most environments. Successful characterizations of the optical properties of fluorescent radicals have been accomplished by lowering the diffusion and recombination rates of the radicals, either by “freezing” the pre-radical in an amorphous solvent glass at cryogenic temperature [28,70,72–74] or by hosting the pre-radical in a solid matrix such as a polymer or a zeolite crystal [27,29,30,75] followed by stimulating radical formation via irradiation, illumination, or thermal exposure. By analogy to these techniques, an amorphous glassy polymer such as epoxy is an environment in which diffusion and recombination

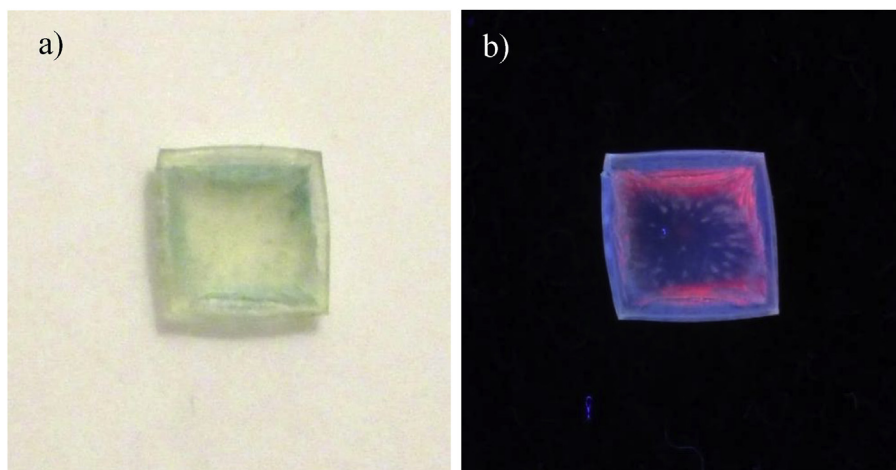


Fig. 6. Images of sample of DGEPPG-DDM after  $\sim 2.5$  GPa true stress compression. a) ambient b) long wave UV.

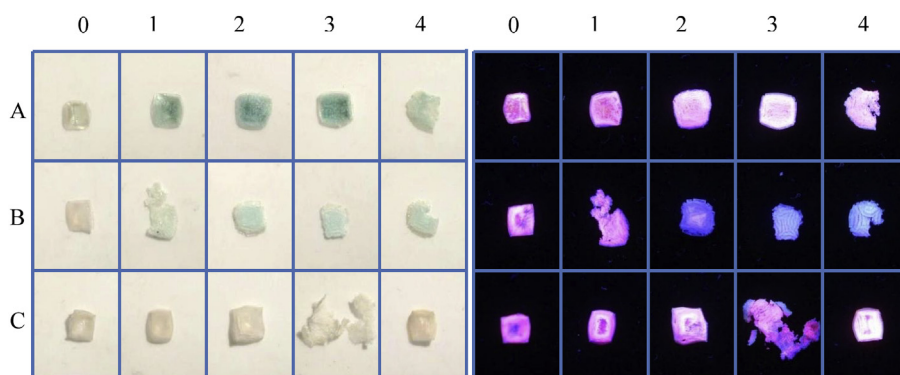


Fig. 7. TGDDM-POPDA samples with controlled d.o.c. after compression to 3000 MPa. Cure conditions (see Table 1) listed at top. left - ambient light. right - long-wave UV light. Row A - excess TGDDM formulation. Row B - balanced formulation. Row C - excess POPDA formulation.

rates of a fluorescent radical should be low, leading to a long life-time and enabling spectroscopic observations.

### 3.4. Analysis of chromophores

In Fig. 3 it is shown that while all DDM-containing formulations displayed similar MRF behavior, some samples showed different MC response. TGDDM-DETA and TGDDM-MMCA, for example, changed from transparent to orange while TGDDM-DDS and DGEBA-DDM changed from transparent to green, while displaying the same “blue-to-red” fluorescence change. To rule out the possibility that green color is generated via some other non-mechanochemical process, we compressed samples such that they show only partial areal activation, to enable spatial correlation observations. Fig. 6 shows ambient-light and fluorescence images of a sample of DGEPPG-DDM compressed to  $\sim 2.5$  GPa of true stress. This sample shows the clear spatial correlation between regions of “red” fluorescence and those of green color formation. The spatial correlation suggests that the green chromophore and red-emitting fluorophore are both created by the same mechanochemical reaction.

To explore the chromophore generation more deeply we eliminated chemistry variation by studying only the TGDDM-POPDA system, and attempted to “drive” MC formulation of one color or the other by varying the stoichiometry and degree of cure of the compressed samples. The degree of cure of samples was determined using Equation (1) to analyze dynamic DSC scans of samples

after the cure conditions recorded in Table 1. The DSC scans are provided in the Supporting Information. Fig. 7 shows the results of this study, with ambient-light images of TGDDM-POPDA samples after 1.5 GPa of compression at left, fluorescent emission of the compressed samples at right. The images are arranged with increasing degree of cure from left to right, and increasing amine stoichiometry from top to bottom.

It is clear that stoichiometry and degree of cure have a large effect on the MC response of the epoxy samples. Samples with incomplete cure of any stoichiometry produce an orange color in response to compression. Compressed samples that are highly cured, with an excess of TGDDM, become green in color. Compressed, highly cured samples with an excess of POPDA become orange in color. Highly cured samples with balanced stoichiometry show very weak green color or no color at all. The fluorescent images show that samples with incomplete cure, or with complete cure of imbalanced stoichiometry, show strong red emission after compression. Balanced, well-cured samples showed increasingly weak fluorescence and very pale green color.

The most dramatic color change resulted from excess TGDDM cure condition 2 (A-2, green) and from excess POPDA condition 4 (C-4, orange). Absorption spectra were collected from these two samples immediately after compression, and then re-measured at increasing times. The spectra collected have been plotted in Fig. 8 along with ambient light and fluorescence images. Both samples showed an initial absorbance peak in the UV with a maximum at  $\sim 365$  nm. After compression both samples showed a strong

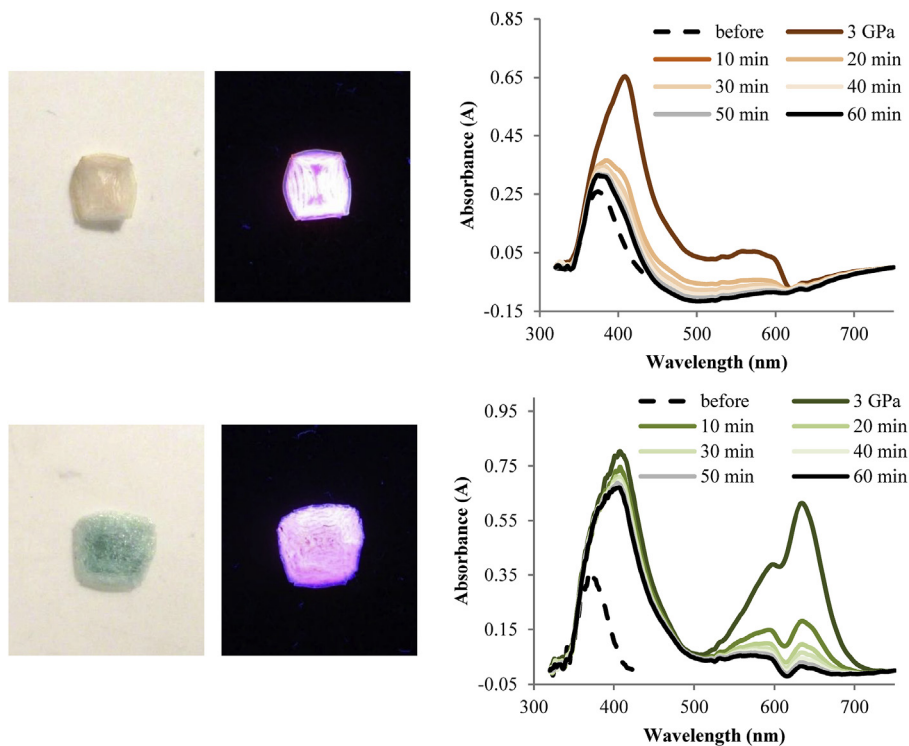


**Fig. 8.** Examples of color formation in TGDDM-POPDA samples – images and absorbance spectra. Top – C-4 (orange). Bottom – A-2 (green). (For interpretation of the references to color in this figure legend, the reader is referred to the Web version of this article.)

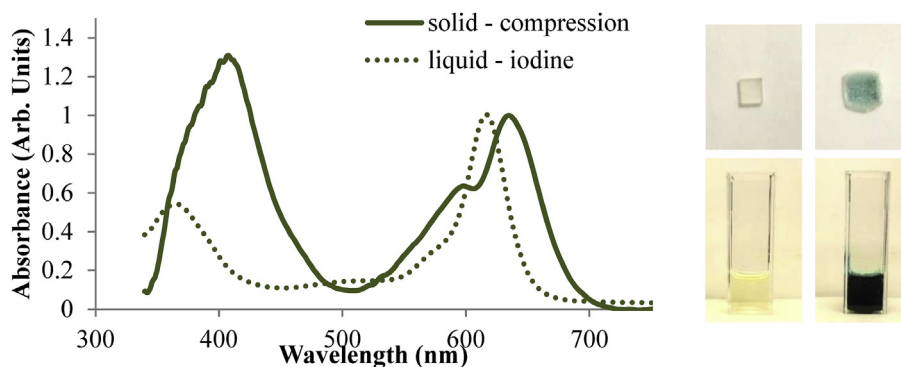


**Fig. 9.** Absorbance spectra of colorful species generated from TGDDM. Solid line - in solid TGDDM-POPDA, via 3GPa compression. Dotted line - in liquid DCM solution, via addition of iodine crystals. Inset images show before and after color change in ambient light. Top – solid via compression; bottom – liquid via iodine. (For interpretation of the references to color in this figure legend, the reader is referred to the Web version of this article.)

increase in absorbance at 410 nm consistent with the excitation spectra assigned to mechanically generated “red”-emitting species in Fig. 2. The green sample also showed a strong increase in absorbance at 635 nm. A notch in the absorbance at 605–610 nm is attributed to the fluorescent emission of the sample in this wavelength region. The colors are transient, fading over the course of a few hours, as reflected in the decrease in absorbance peaks as time increases.

This analysis serves as further evidence that the orange chromophore is also the “red”-emitting fluorophore. Absorbance at 410 nm, shown in Fig. 2 to be the excitation responsible for red emission, is present in both orange and green-colored samples; the 635 nm-absorbing green chromophore cannot be the fluorophore since it is not present in sample C-4 which is strongly red fluorescent. However, samples that appear green may also have orange chromophores present, as evidenced by strong 410 nm absorbance

from the green-appearing sample A-2. This also suggests that the orange and green chromophores are not mutually exclusive.

Our observations of the dependence on degree of cure and stoichiometry of the colors developed after compression are consistent with the behavior of persistent radicals. The absorbance of the cation of diphenylmethyl radical is at much higher wavelength than the radical itself, and the equilibrium between radical and cation form can be influenced by the pH or presence of oxidizing gases in the environment, or thermally [29,76]. The stoichiometric changes to the formulations of TGDDM-POPDA, and the modifications of degree of cure, change the concentration of unreacted amines and epoxides which modify the electron-donating character of the environment around a formed radical and favor either the orange benzoidal radical or the green quinoidal form.

The formation of the green chromophore can be investigated

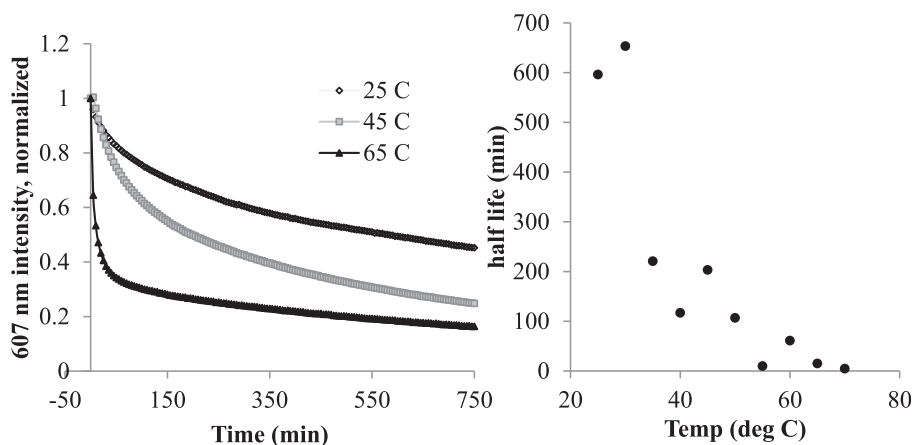


**Fig. 10.** a) Intensity of 607 nm emission peak vs time for TGDDM-DETA samples after 1.5 GPa compression, measured at various temperatures. b) Half-life of intensity decay vs measurement temperature.

**Table 1**

Cure process, degree of cure (d.o.c.), and  $T_g$  for TGDDM-POPDA formulations.

Condition	0	1	2	3	4
Cure process	RT 24hr, 50 °C 1hr	Condition 0 + 75 °C 30min	Condition 0 + 100 °C 30min	Condition 0 + 125 °C 30min	Condition 0 + 150 °C 30min
A d.o.c. ( $T_g$ , °C)	.87	.98 (49.5)	1 (54.7)	1 (61.0)	1 (63.4)
B d.o.c. ( $T_g$ , °C)	.70	.89 (59.0)	1 (80.8)	1 (95.5)	1 (98.5)
C d.o.c. ( $T_g$ , °C)	.88	.99 (51.2)	1 (61.6)	1 (65.6)	1 (68.3)

further by experiments in solution. Fig. 9 shows absorbance spectra of a TGDDM-POPDA sample demonstrating green color change due to compression, compared with a similar green color can be observed in a 5 wt% TGDDM solution in DCM after the addition of a few grains of iodine solid and brief sonication. The samples have a strong absorbance peak at ~615–635 nm; a peak at 410 nm is observable in the solid samples but not in liquid, which has a small peak at 365 nm. The images inset to Fig. 9 show before and after ambient light images of the color change. When illuminated by 390 nm excitation, the solid sample was highly fluorescent while the liquid was not.

Aromatic amines such as DDM are known to oxidize to quinoidal methine form with iodine in solution, often producing strong visible absorption [77–80]. The similarity in absorbance between the TGDDM-DCM-iodine solution and the solid TGDDM-POPDA sample after compression is strong evidence that a similar quinoidal methine is formed in response to compression via some mechanochemical intramolecular reaction. The solid sample also exhibits 410 nm absorbance and 607 nm emission, while the liquid sample has neither. This supports the correlation in Fig. 2 between 410 nm excitation peak and 607 nm emission from samples after compression. The presence of the green chromophore in the liquid sample in the absence of 607 nm fluorescence suggests that the green chromophore is not fluorescent at room temperature in liquid DCM.

### 3.5. Time stability after activation

The “red” fluorescent emission observed in Figs 2–4 is not permanent – illumination with identical UV excitation produces successively lower emission intensities over time. The decrease in “red” emission intensity is not accompanied by an increase in “blue” emission intensity, meaning the decrease is not due to a reversal of the “blue-to-red” transition but a further conversion of the “red” fluorophore to some non-emissive state. This conversion is more rapid if the sample is held at elevated temperatures. Fig. 10a

shows time resolved measurements of the “red” fluorescent emission intensity measured from TGDDM-POPDA samples at increasing times after 1.5 GPa of compressive true stress, taken from samples held at temperatures from 25 to 70 °C. Fig. 10b shows the intensity half-lives for different temperatures. The emission intensities have been normalized to the intensity value at the onset of measurement, which was ~5 min after unloading the sample. The emission intensity decreases with time; increasing the temperature of the sample during measurement increases the rate of decrease.

We attribute the decrease in emission intensity of the “red” fluorescence over time to a conversion of the compression-generated reactive intermediate fluorophore to some non-emissive product. The companion work to this report demonstrates that high-intensity UV illumination serves to activate the “red” fluorescence rather than quench it – this rules out photobleaching or photo-oxidation effects as the reason for the emission intensity decay. The increasing rate of decay with increasing temperature is consistent with a diffusion-dependent recombination reaction, which is one pathway for a reactive intermediate “red” fluorophore to become non-emissive [10,81,82]. Other pathways to non-emissive species include oxidation reactions to produce carbonyls and formation of quinoidal methines.

The traditional method of studying radical species is EPR spectroscopy. EPR studies of mechanically deformed samples of TGDDM-DETA epoxy confirm that large quantities of radicals are produced in compression compared to undeformed samples. Similar results were obtained from photo-activated samples of TGDDM-POPDA, which are discussed in the companion work. Fig. 11 shows the EPR spectra of a sample of TGDDM-DETA collected before compression and at increasing times after compression to ~7 GPa true stress, over the course of several days. The spectra collected after compression used a quartz insert and had a different microwave frequency, which accounts for the shift in center crossing point and differences in signal to noise ratio. The  $g$  values of 2.007–2.008 from samples before and after compression indicate the presence of organic radicals, with a large increase in radical

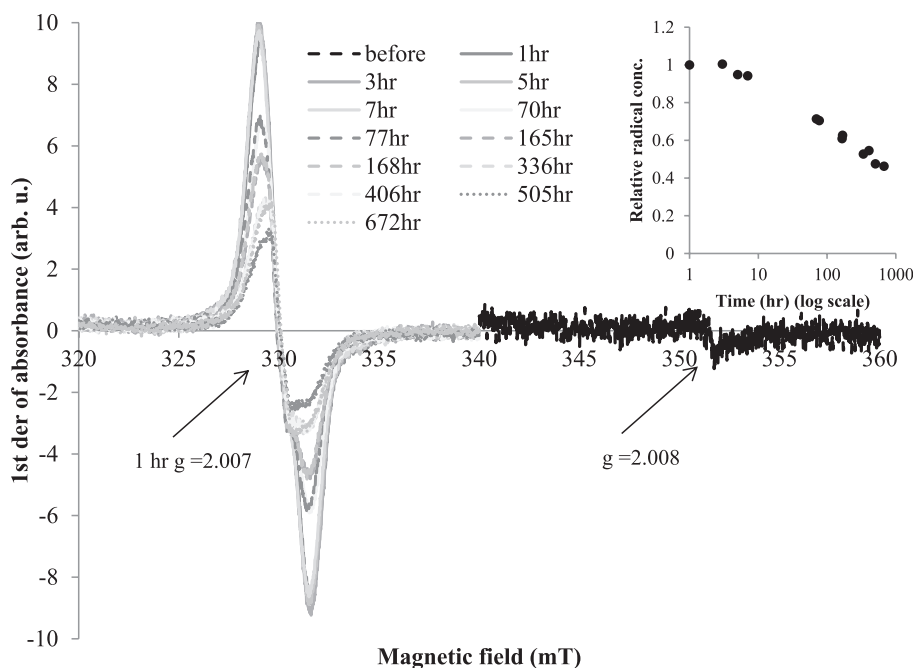


**Fig. 11.** EPR spectra of TGDDM-DETA sample before compression and at various times after compression. Inset: relative radical concentration vs time after compression, time axis logarithmic.

concentration after compression. Over time the relative radical concentration decreases in a manner consistent with a first-order decay reaction, as plotted in the inset to Fig. 11. The EPR spectrum of the compressed epoxy does not display hyperfine structure suitable for positive identification of the radical, however its general shape and features are quite similar to those observed by researchers creating radicals in epoxy using other stimuli [14,16,83–87]. There appear to be two overlapping spectral

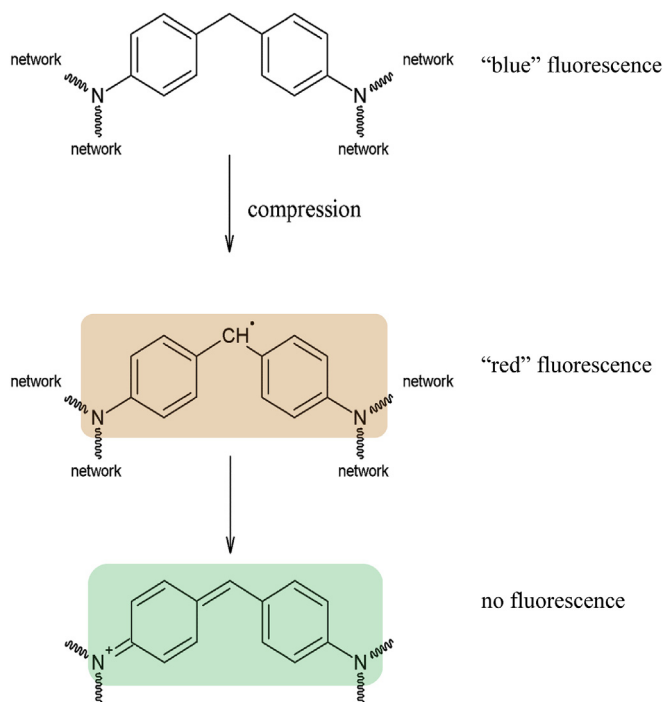
contributions, with different decay rates. This is consistent with other observations of radicals in epoxy as well [87]. Epoxy samples that were made fluorescent via photo-activation also showed a large increase in radical concentration, with EPR signal indistinguishable from that displayed by mechanically activated samples. This work is discussed in more detail in the companion work.

### 3.6. Mechanism

Scheme 1 presents the original DDM structure, the reactive intermediate structure, and a quinoidal methine structure, which are responsible for the color and fluorescence changes in DDM-containing epoxies. Mechanically induced bond scission at any of several adjacent bonds to the DDM structure, including the C-N crosslink bonds, may result in radicals which ultimately migrate to the central methylene of the DDM structure. This radical structure can reduce its energy via resonance, making it preferable for delocalized radical charge. A radical on the DDM structure in an amorphous glassy thermoset environment such as cured epoxy may be expected to have orange color, red fluorescence, and relatively long lifetime consistent with our observations. As proposed by others to account for the green coloration observed, the quinoidal methine structure of DDM is a natural structure to form from the DDM central methylene radical. The selection of orange form or green form as the preferred structure for the different formulations will be studied in future works.

## 4. Conclusions

This paper presents our study of the mechanochromic and mechanoresponsive fluorescence properties of diamine-cured epoxy formulations containing the diaminodiphenylmethane structure. Such epoxies displayed an irreversible “blue-to-red” change in fluorescence emission when uniaxially compressed. The activation of this change occurs in the early stages of strain hardening, consistent with bond scission. The fluorescence change is accompanied by the formation of orange and green chromophores;



**Scheme 1.** Scheme for reactions creating orange and green chromophores and red fluorophore in DDM-containing epoxies.

spectroscopic evidence shows the orange chromophore is the red-emitting fluorophore, its EPR spectrum and impermanent emission in time show it to be a reactive intermediate formed by compression-initiated bond scission events. One product of such events is the quinoidal methine form of DDM, which is shown here to be the green mechanochemically generated chromophore.

## Acknowledgements

Dr. Jen would like to thank the Boeing-Johnson Foundation for its support.

## Appendix A. Supplementary data

Supplementary data related to this article can be found at <https://doi.org/10.1016/j.polymer.2018.03.029>.

## References

- [1] D.R.T. Roberts, S.J. Holder, Mechanochromic systems for the detection of stress, strain and deformation in polymeric materials, *J. Mater. Chem.* 21 (2011) 8256, <https://doi.org/10.1039/c0jm04237d>.
- [2] D.A. Davis, A. Hamilton, J. Yang, L.D. Cremer, D. Van Gough, S.L. Potisek, et al., Force-induced activation of covalent bonds in mechanoresponsive polymeric materials, *Nature* 459 (2009) 68–72, <https://doi.org/10.1038/nature07970>.
- [3] D.A. Davis, Spiropyran as Color-generating Mechanophores, University of Illinois at Urbana-Champaign, 2010. <http://hdl.handle.net/2142/16933>.
- [4] Z. Chi, X. Zhang, B. Xu, X. Zhou, C. Ma, Y. Zhang, et al., Recent advances in organic mechanochromic materials, *Chem. Soc. Rev.* 41 (2012) 3878, <https://doi.org/10.1039/c2cs35016e>.
- [5] C. Löwe, C. Weder, Oligo(p-phenylene vinylene) excimers as molecular probes: deformation-induced color changes in photoluminescent polymer blends, *Adv. Mater.* 14 (2002) 1625–1629, [https://doi.org/10.1002/1521-4095\(20021118\)14:22<1625::AID-ADMA1625>3.0.CO;2-Q](https://doi.org/10.1002/1521-4095(20021118)14:22<1625::AID-ADMA1625>3.0.CO;2-Q).
- [6] C. Weder, Mechanoresponsive materials, *J. Mater. Chem.* 21 (2011) 8235, <https://doi.org/10.1039/c1jm90068d>.
- [7] M. Zhao, L. Meng, L. Ma, L. Ma, X. Yang, Y. Huang, et al., Layer-by-layer grafting CNTs onto carbon fibers surface for enhancing the interfacial properties of epoxy resin composites, *Compos. Sci. Technol.* 154 (2018) 28–36, <https://doi.org/10.1016/j.compscitech.2017.11.002>.
- [8] C. Wang, M. Zhao, J. Li, J. Yu, S. Sun, S. Ge, et al., Silver nanoparticles/graphene oxide decorated carbon fiber synergistic reinforcement in epoxy-based composites, *Polym. (United Kingdom)* 131 (2017) 263–271, <https://doi.org/10.1016/j.polymer.2017.10.049>.
- [9] Z. Li, R. Toivola, F. Ding, J. Yang, P.-N.N. Lai, T. Howie, et al., Highly sensitive built-in strain sensors for polymer composites: fluorescence turn-on response through mechanochemical activation, *Adv. Mater.* 28 (2016) 6592–6597, <https://doi.org/10.1002/adma.201600589>.
- [10] R. Toivola, P.-N. Lai, J. Yang, S.-H. Jang, A.K.-Y. Jen, B.D. Flinn, Mechanochromic fluorescence in epoxy as a detection method for barely visible impact damage in CFRP composites, *Compos. Sci. Technol.* 139 (2017) 74–82, <https://doi.org/10.1016/j.compscitech.2016.11.026>.
- [11] S.Y. Cho, J.G. Kim, C.M. Chung, A fluorescent crack sensor based on cyclobutane-containing crosslinked polymers of tricinamates, *Sensor. Actuator. B Chem.* 134 (2008) 822–825, <https://doi.org/10.1016/j.snb.2008.06.042>.
- [12] J. Zou, Y. Liu, B. Shan, A. Chattopadhyay, L.L. Dai, Early damage detection in epoxy matrix using cyclobutane-based polymers, *Smart Mater. Struct.* 23 (2014) 95038, <https://doi.org/10.1088/0964-1726/23/9/095038>.
- [13] E.M. Nofen, J. Wickham, B. Koo, A. Chattopadhyay, L.L. Dai, Dimeric anthracene-based mechanophore particles for damage precursor detection in reinforced epoxy matrix composites, *Mater. Res. Express* 3 (2016) 35701, <https://doi.org/10.1088/2053-1591/3/3/035701>.
- [14] M.I. Fulton, P.J. Pomery, N.A.S. John, G.A. George, Colour development and luminescence phenomena in epoxy glasses, *Polym. Adv. Technol.* 9 (1998) 75–83.
- [15] V. Bellenger, J. Verdu, Photooxidation of amine crosslinked epoxies I. The DGEBA-DDM system, *J. Appl. Polym. Sci.* 28 (1983) 2599–2609.
- [16] N.M. Atherton, L.G. Banks, B. Ellis, Development of Green and dark blue colors in epoxy resins cured with 4,4'-diaminodiphenylmethane, *J. Appl. Polym. Sci.* 27 (1982) 2015–2023.
- [17] B. Mailhot, S. Morlat-Thérias, M. Ouahioune, J.L. Gardette, Study of the degradation of an epoxy/amine resin, 1 photo- and thermo-chemical mechanisms, *Macromol. Chem. Phys.* 206 (2005) 575–584, <https://doi.org/10.1002/macp.200400395>.
- [18] N.S. Allen, J.P. Binkley, B.J. Parsons, G.O. Phillips, N.H. Tennent, Spectroscopic properties and photosensitivity of epoxy resins, *Polym. Photochem.* 2 (1982) 97–107, [https://doi.org/10.1016/0144-2880\(82\)90033-1](https://doi.org/10.1016/0144-2880(82)90033-1).
- [19] R.L. Clough, K.T. Gillen, G.M. Malone, J.S. Wallace, Color formation in irradiated polymers, *Radiat. Phys. Chem.* 48 (1996) 583–594, [https://doi.org/10.1016/0969-806X\(96\)00075-8](https://doi.org/10.1016/0969-806X(96)00075-8).
- [20] A. Ruiz de Luzuriaga, J.M. Matxain, F. Ruipérez, R. Martín, J.M. Asua, G. Cabañero, et al., Transient mechanochromism in epoxy vitrimer composites containing aromatic disulfide crosslinks, *J. Mater. Chem. C* 4 (2016) 6220–6223, <https://doi.org/10.1039/C6TC02383E>.
- [21] C. Galant, B. Fayolle, M. Kuntz, J. Verdu, Thermal and radio-oxidation of epoxy coatings, *Prog. Org. Coatings* 69 (2010) 322–329, <https://doi.org/10.1016/j.porgcoat.2010.07.005>.
- [22] V. Bellenger, J. Verdu, Photooxidation of amine crosslinked epoxies II. Influence of structure, *J. Appl. Polym. Sci.* 28 (1983) 2677–2688.
- [23] R.L. Levy, D.P. Ames, Effect of sorbed water on epoxy fluorescence, in: *Polym. Mater. Sci. Eng. - Proc. ACS Div. Polym. Mater. Sci. Eng.*, 53, American Chemical Society, Chicago, IL, 1985, pp. 176–179.
- [24] R.L. Levy, Viscosity-dependent self-probe fluorescence of an epoxy resin, in: *Polym. Mater. Sci. Eng. - Proc. ACS Div. Polym. Mater. Sci. Eng.*, 50, American Chemical Society, St. Louis, MO, 1984, pp. 124–129.
- [25] R.L. Levy, D.P. Ames, Monitoring epoxy cure kinetics with a viscosity-dependent fluorescence probe, in: *Org. Coatings Appl. Polym. Sci. - Proc. ACS Div. Org. Coatings Plast. Chem.*, 48, American Chemical Society, Seattle, WA, 1983, pp. 116–120.
- [26] A. Bromberg, K.H. Schmidt, D. Meisel, Photochemistry and photophysics of phenylmethyl radicals, *J. Am. Chem. Soc.* 106 (1984) 3056–3057.
- [27] H. Namai, H. Ikeda, Y. Hoshii, N. Kato, Y. Morishita, K. Mizuno, Thermoluminescence and a new organic light-emitting diode (OLED) based on triplet-triplet fluorescence of the trimethylenemethane (TMM) biradical, *J. Am. Chem. Soc.* 129 (2007) 9032–9036, <https://doi.org/10.1021/ja070946+>.
- [28] E. Whittle, D.A. Dows, G.C. Pimentel, Matrix isolation method for the experimental study of unstable species, *J. Chem. Phys.* 22 (1954) 1943.
- [29] S. Jockusch, T. Hirano, Z.Q. Liu, N.J. Turro, A spectroscopic study of diphenylmethyl radicals and diphenylmethyl carbocations stabilized by zeolites, *J. Phys. Chem. B* 104 (2000) 1212–1216, <https://doi.org/10.1021/jp992978s>.
- [30] Hiroshi Ikeda, An organic radical light-emitting diode based on the fluorescence emission of a trimethylenemethane biradical, *J. Photopolym. Sci. Technol.* 21 (2008) 327–332.
- [31] Y. Hattori, T. Kusamoto, H. Nishihara, Luminescence, stability, and proton response of an open-shell (3,5-Dichloro-4-pyridyl)bis(2,4,6-trichlorophenyl)methyl radical, *Angew. Chemie - Int. Ed.* 53 (2014) 11845–11848, <https://doi.org/10.1002/anie.201407362>.
- [32] L. Michaelis, M.P. Schubert, S. Granick, The free radicals of the type of Wurster's salts, *J. Am. Chem. Soc.* 61 (1939) 1981–1992, <https://doi.org/10.1021/ja01877a013>.
- [33] H. Hoa, H.M. Solomon, M. Taguchi, T. Kojima, Polyvinyl Butyral Films Containing Leuco-malachite green as Low-dose Dosimeters, 77, 2008, pp. 457–462, <https://doi.org/10.1016/j.radphyschem.2007.06.012>.
- [34] J. Allen, J.R. Meinertz, Post-column reaction for simultaneous analysis of chromatic and leuco forms of malachite green and crystal violet by high-performance liquid chromatography with photometric detection, *J. Chromatogr.* 536 (1991) 217–222.
- [35] Q. Sui, X.-T. Ren, Y.-X. Dai, K. Wang, W. Li, T. Gong, et al., Piezochromism and hydrochromism through electron transfer: new stories for viologen, *Chem. Sci.* 8 (2017) 2758–2768, <https://doi.org/10.1039/C6SC04579K>.
- [36] T. He, N. Niu, Z. Chen, S. Li, S. Liu, J. Li, Novel quercetin aggregation-induced emission luminogen (AIEgen) with excited-state intramolecular proton transfer for in vivo bioimaging, *Adv. Funct. Mater.* 1706196 (2018) 1–7, <https://doi.org/10.1002/adfm.201706196>.
- [37] C.R. Hickenboth, J.S. Moore, S.R. White, N.R. Sottos, J. Baudry, S.R. Wilson, Biasing reaction pathways with mechanical force, *Nature* 446 (2007) 423–427, <https://doi.org/10.1038/nature05681>.
- [38] P. Dopieralski, P. Anjukandi, M. Rückert, M. Shiga, J. Ribas-Arino, D. Marx, On the role of polymer chains in transducing external mechanical forces to benzocyclobutene mechanophores, *J. Mater. Chem.* 21 (2011) 8309–8316, <https://doi.org/10.1039/C0JM03698F>.
- [39] M. Wollenhaupt, M. Krupicka, D. Marx, Should the Woodward-Hoffmann rules be applied to mechanochemical reactions? *ChemPhysChem* (2015) 1593–1597, <https://doi.org/10.1002/cphc.201500054>.
- [40] M.T. Ong, The Photochemical and Mechanochemical Ring Opening of Cyclobutene from First Principles, University of Illinois at Urbana-Champaign, 2010.
- [41] J. Saltiel, L.-S. Ng-Lim, Stereospecific photochemical fragmentation of cyclobutenes in solution, *J. Am. Chem. Soc.* 91 (1969) 5404–5405.
- [42] K.B. Clark, W.J. Leigh, Cyclobutene photochemistry. Nonstereospecific photochemical ring opening of simple cyclobutenes, *J. Am. Chem. Soc.* 109 (1987) 6086–6092, <https://doi.org/10.1021/ja00254a030>.
- [43] V.I. Minkin, Photo-, thermo-, solvato-, and electrochromic spiroheterocyclic compounds, *Chem. Rev.* 104 (2004) 2751–2776, <https://doi.org/10.1021/cr020088u>.
- [44] R. Heiligman-Rim, Y. Hirshberg, E. Fischer, Photochromism in spiropyran. Part IV. Evidence for the existence of several forms of the colored modification, *J. Phys. Chem.* 66 (1962) 2465–2470.
- [45] F. Wilkinson, D. Reeves, Photochromism of spiropyran, *J. Chem. Soc., Faraday Trans. 2* (69) (1973) 1381–1390.
- [46] E.F.R. Heiligman-Rim, Y. Hirshberg, Photochromism in spiropyran. Part V. On the mechanism of phototransformation, *J. Phys. Chem.* 66 (1962) 2470–2477, <https://doi.org/10.1021/j100818a036>.
- [47] K. Maeda, T. Hayashi, Photochromic color change of the dimer of triphenylimidazolyl at low temperatures, *Bull. Chem. Soc. Jpn* 1563 (1969) 3509–3514,

- <https://doi.org/10.1246/bcsj.42.3509>.
- [48] K. Maeda, T. Hayashi, The mechanism of photochromism, thermochromism and piezochromism of dimers of triarylimidazolyl, *Bull. Chem. Soc. Jpn* 43 (1970) 429–438, <https://doi.org/10.1246/bcsj.43.429>.
- [49] F. Verstraeten, R. Göstl, R.P. Sijbesma, Stress-induced colouration and cross-linking of polymeric materials by mechanochemical formation of triphenylimidazolyl radicals, *Chem. Commun* 52 (2016) 8608–8611, <https://doi.org/10.1039/C6CC04312G>.
- [50] G.A. George, D.P. Schweinsberg, Characterization of the cure of TGDDM/DDC epoxy resins by chemiluminescence I. Spectral and thermal analysis, *J. Appl. Polym. Sci.* 33 (1987) 2281–2292.
- [51] O. Gallot-lavallée, G. Teysse, C. Laurent, S. Rowe, Identification of photoluminescence features of an epoxy resin based on components features and curing effects, *Polymer (Guildf)* 46 (2005) 2722–2731, <https://doi.org/10.1016/j.polymer.2005.02.003>.
- [52] J.C. Moller, S.A. Barr, E.J. Schultz, T.D. Breitzman, R.J. Berry, Simulation of fracture nucleation in cross-linked polymer networks, *Jom* 65 (2013) 147–167, <https://doi.org/10.1007/s11837-012-0511-1>.
- [53] M.A. Grayson, C.J. Wolf, Mechanochemical reactions in an epoxy resin system, *J. Polym. Sci. Polym. Phys. Ed.* 23 (1985) 1087–1097, <https://doi.org/10.1002/pol.1985.180230601>.
- [54] J.T. Dickinson, L.C. Jensen, S.K. Bhattacharya, Fracto-emission from neat epoxy resin, *Makromolekulare Chemie, Macromol. Symp* (1987) 129–152.
- [55] J. Sohma, M. Sakaguchi, ESR studies on polymer radicals produced by mechanical destruction and their reactivity, *New Sci. Adv. Polym. Sci.* 20 (1976) 109–158, <https://doi.org/10.1007/BFb0023970>.
- [56] M.D. Glad, E.J. Kramer, Microdeformation and network structure in epoxies, *J. Mater. Sci.* 26 (1991) 2273–2286.
- [57] J.C. Moller, S.A. Barr, T.D. Breitzman, G.S. Kedziora, A.M. Ecker, R.J. Berry, et al., Prediction of incipient nano-scale rupture for thermosets in plane stress, *Fract. Fatigue, Fail. Damage Evol.* 8 (2016) 253–260, <https://doi.org/10.1007/978-3-319-21611-9>.
- [58] S.A. Barr, G.S. Kedziora, A.M. Ecker, J.C. Moller, R.J. Berry, T.D. Breitzman, Bond breaking in epoxy systems: a combined QM/MM approach, *J. Chem. Phys.* 144 (2016) 244904, <https://doi.org/10.1063/1.4954507>.
- [59] L.M. Pisarenko, A.B. Gagarina, V.A. Roginskii, Mechanochromic effect and the formation of free radicals in bis(phenylphthaloyl)ethane dimers upon mechanical destruction in the solid phase, *Bull. Acad. Sci. USSR Div. Chem. Sci.* 36 (1987) 2658–2660, <https://doi.org/10.1007/BF00957263>.
- [60] J.M. Lenhardt, M.T. Ong, R. Choe, C.R. Evenhuis, T.J. Martinez, S.L. Craig, Trapping a diradical transition state by mechanochemical polymer extension, *Science* 329 (2010) 1057–1060, <https://doi.org/10.1126/science.1193412>.
- [61] K. Imato, A. Irie, T. Kosuge, T. Ohishi, M. Nishihara, A. Takahara, et al., Mechanochemistry with a reversible radical system and freezing-induced mechanochemistry in polymer solutions and gels, *Angew. Chem. - Int. Ed.* 54 (2015) 6168–6172, <https://doi.org/10.1002/anie.201412413>.
- [62] M. Abe, H. Furunaga, D. Ma, L. Gagliardi, G.J. Bodwell, Stretch effects induced by molecular strain on weakening sigma-bonds: molecular design of long-lived diradicals (biradicals), *J. Org. Chem.* 77 (2012) 7612–7619.
- [63] H. Hiratsuka, T. Yamazaki, T. Hikida, Y. Mori, Visible absorption and fluorescence spectra of the benzalacetophenone ketyl radical and its radical anion, *J. Chem. Soc. Faraday Trans.* 80 (1984) 861–866.
- [64] H. Hiratsuka, T. Yamazaki, Y. Maekawa, Y. Kajii, T. Hikida, Y. Mori, Fluorescence spectra and lifetimes of chalcone ketyl radical anions, *Chem. Phys. Lett.* 139 (1987) 187–190.
- [65] K. Obi, H. Yamaguchi, Fluorescence lifetime and quantum yield of diphenylketyl radical at low temperature, *Chem. Phys. Lett.* 54 (1978) 448–450.
- [66] M. Sakamoto, X. Cai, M. Hara, S. Tojo, M. Fujitsuka, T. Majima, Transient absorption spectra and lifetimes of benzophenone ketyl radicals in the excited state transient absorption spectra and lifetimes of benzophenone ketyl radicals in the excited state, *J. Phys. Chem. A* 108 (2004) 8147–8150, <https://doi.org/10.1021/jp047058a>.
- [67] A.R. Cook, L.A. Curtiss, J.R. Miller, Fluorescence of the 1,4-benzoquinone radical anion, *J. Am. Chem. Soc.* 119 (1997) 5729–5734, <https://doi.org/10.1021/ja970270q>.
- [68] T. Kusamoto, S. Kimura, Y. Ogino, C. Ohde, H. Nishihara, Modulated luminescence of a stable open-shell triarylmethyl radical: effects of chemical modification on its electronic structure and physical properties, *Chem. - A Eur. J* (2016) 1–10, <https://doi.org/10.1002/chem.201602942>.
- [69] Y. Hattori, T. Kusamoto, H. Nishihara, Highly photostable luminescent open-shell (3,5-dihalo-4-pyridyl)bis(2,4,6-trichlorophenyl)methyl radicals: significant effects of halogen atoms on their photophysical and photochemical properties, *RSC Adv* 5 (2015) 64802–64805, <https://doi.org/10.1039/C5RA14268G>.
- [70] A. Bromberg, D. Meisel, Photophysics of arylmethyl radicals at 77 K. Structure-photoreactivity correlation, *J. Phys. Chem.* 89 (1985) 2507–2513, <https://doi.org/10.1021/j100258a017>.
- [71] L.J. Johnston, Photochemistry of radicals and biradicals, *Chem. Rev.* 93 (1995) 251–266, <https://doi.org/10.1021/cr00017a012>.
- [72] I. Norman, G. Porter, Trapped atoms and radicals in a glass “cage”, *Nature* 174 (1954) 508–509, <https://doi.org/10.1038/174508a0>.
- [73] I. Norman, G. Porter, Trapped atoms and radicals in rigid solvents, *Proc. R. Soc. Part A* 230 (1955) 399.
- [74] P. Brodard, A. Sarbach, J. Gumy, T. Bally, E. Vauthey, Excited-state dynamics of organic radical ions in liquids and in low-temperature matrices, *J. Phys. Chem. A* 105 (2001) 6594–6601.
- [75] S. Hashimoto, Zeolite photochemistry: impact of zeolites on photochemistry and feedback from photochemistry to zeolite science, *J. Photochem. Photobiol. C Photochem. Rev.* 4 (2003) 19–49, [https://doi.org/10.1016/S1389-5567\(03\)00003-0](https://doi.org/10.1016/S1389-5567(03)00003-0).
- [76] T. Hirano, W. Li, L. Abrams, P.J. Krusic, M.F. Ottaviani, N.J. Turro, Reversible oxygenation of a diphenylmethyl radical rendered supramolecularly persistent [11], *J. Am. Chem. Soc.* 121 (1999) 7170–7171, <https://doi.org/10.1021/ja9912628>.
- [77] H. Tsubomura, Molecular complexes and their spectra. X. Molecular complexes between iodine and N,N-Dimethylaniline derivatives, *J. Am. Chem. Soc.* 82 (1960) 40–45, <https://doi.org/10.1021/ja01486a010>.
- [78] H. Kusakawa, S. Nishizaki, Ultraviolet and visible absorption spectra of the solid of aromatic amine complexes with iodine, *Bull. Chem. Soc. Jpn* 38 (1965) 783.
- [79] R. Foster, The absorption spectra of molecular complexes, *Tetrahedron* 10 (1960) 96–101.
- [80] P. Aravindan, P. Maruthamuthu, P. Dharmalingam, Stopped-flow kinetic study of the formation and decay of the 4,4'-(dimethylamino)diphenylmethane radical cation in aqueous solution, *J. Chem. Soc. Faraday Trans.* 91 (1995) 2743–2749.
- [81] T.R. Waite, General theory of bimolecular reaction rates in solids and liquids, *J. Chem. Phys.* 28 (1958) 103–106, <https://doi.org/10.1063/1.1744051>.
- [82] S. Shimada, Y. Hori, H. Kashiwabara, Free radicals trapped in polyethylene matrix: 2. Decay in single crystals and diffusion, *Polymer (Guildf)* 18 (1977) 25–31, [https://doi.org/10.1016/0032-3861\(77\)90257-9](https://doi.org/10.1016/0032-3861(77)90257-9).
- [83] S.G. Burnay, Radiation-induced changes in the structure of an epoxy resin, *Radiat. Phys. Chem.* 16 (1980) 389–397, [https://doi.org/10.1016/0146-5724\(80\)90235-6](https://doi.org/10.1016/0146-5724(80)90235-6).
- [84] B. Eda, M. Iwasaki, An ESR study of radiation damage in bisphenol-A-based epoxy resin at low temperature: selective hydrogen addition to benzene-ring-forming cyclohexadienyl-type radical, *J. Polym. Sci. Part A Polym. Chem.* 24 (1986) 2119–2129, <https://doi.org/10.1002/cne.902970204>.
- [85] K. Shirane, Radiation-induced free radicals of epoxy resin, *J. Polym. Sci. Polym. Lett. Ed.* 17 (1979) 139–142, <https://doi.org/10.1002/cne.902970204>.
- [86] K.R. Schaffer, R.E. Fornes, R.D. Gilbert, J.D. Memory, Electron spin resonance study of a cured epoxy resin exposed to high-energy radiation, *Polymer (Guildf)* 25 (1984) 54–56, [https://doi.org/10.1016/0032-3861\(84\)90266-0](https://doi.org/10.1016/0032-3861(84)90266-0).
- [87] K.S. Seo, R.E. Fornes, R.D. Gilbert, J.D. Memory, Effects of ionizing radiation on epoxy, graphite fiber, and epoxy/graphite fiber composites. Part II: radical types and radical decay behavior, *J. Polym. Sci. Part B Polym. Phys.* 26 (1988) 533–544, <https://doi.org/10.1002/cne.902970204>.